



HHS Public Access

Author manuscript

Nat Commun. Author manuscript; available in PMC 2016 April 12.

Published in final edited form as:

Nat Commun. ; 6: 8565. doi:10.1038/ncomms9565.

Migration of Germline Progenitor Cells is Directed by Sphingosine-1-Phosphate Signaling in a Basal Chordate

Susannah H. Kassmer^{*,1,2}, Delany Rodriguez¹, Adam D. Langerbacher², Connor Bui², and Anthony W. De Tomaso²

¹Neuroscience Research Institute, University of California, Santa Barbara, CA 93106, USA

²Molecular, Cellular and Developmental Biology, University of California, Santa Barbara, CA 93106, USA

Abstract

The colonial ascidian *Botryllus schlosseri* continuously regenerates entire bodies in an asexual budding process. The germ line of the newly developing bodies is derived from migrating germ cell precursors, but the signals governing this homing process were unknown. Here we show that germ cell precursors can be prospectively isolated based on expression of aldehyde dehydrogenase and integrin alpha 6, and that these cells express germ cell markers such as *vasa*, *pumilio* and *piwi*, as well as *sphingosine-1-phosphate receptor*. *In vitro*, sphingosine-1-phosphate (S1P) stimulates migration of germ cells, which depends on integrin-alpha-6-activity. *In vivo*, S1P signaling is essential for homing of germ cells to newly developing bodies. S1P is generated by sphingosine kinase in the developing germ cell niche and degraded by lipid phosphate phosphatase in somatic tissues. These results demonstrate a previously unknown role of the S1P signaling pathway in germ cell migration in the ascidian *Botryllus schlosseri*.

Keywords

Germ cells; cell migration; sphingosine-1-phosphate

Introduction

In most organisms, germ cells are specified early in development, and must migrate through and along various somatic tissues to reach the somatic niche of the gonad. In contrast to somatic tissues, which cease to exist when an organism dies, germ cells link successive

Users may view, print, copy, and download text and data-mine the content in such documents, for the purposes of academic research, subject always to the full Conditions of use:http://www.nature.com/authors/editorial_policies/license.html#terms

*Corresponding author: Correspondence to: Susannah.kassmer@lifesci.ucsb.edu.

Competing Financial Interests Statement:

The authors declare no competing financial interests.

Author contributions

SHK: Study conception and design, acquisition of data, analysis and interpretation of data, drafting of manuscript, critical revision of manuscript, final approval of manuscript. DR: acquisition of data, analysis and interpretation of data, critical revision of manuscript, final approval of manuscript. ADL: analysis and interpretation of data, critical revision of manuscript, final approval of manuscript. CB: acquisition of data. AWD: Study conception and design, analysis and interpretation of data, critical revision of manuscript, final approval of manuscript.

generations together, and are, in that sense, immortal (reviewed in ¹). Ascidians are marine invertebrate chordates that straddle the evolutionary divide between invertebrates and vertebrates. Embryogenesis results in a swimming tadpole larva with characteristic chordate features that later undergoes metamorphosis into a sessile invertebrate adult. Colonial ascidian species increase in size via an asexual budding process, during which their entire bodies, including all somatic and germline tissues, are regenerated *de novo*. Colonies of *Botryllus schlosseri* asexually reproduce every week, within a 2-3 year lifespan, providing a unique model to study asexual reproduction and regeneration ². Individuals within the colony are interconnected by a shared, extracorporeal vasculature, and are embedded in an extracellular matrix known as the tunic. Two generations of newly developing bodies, termed primary and secondary buds (Figure 1A) grow from the adult bodies, known as zooids. Secondary buds begin as small protrusions of the body wall of primary buds, and proceed to form a closed vesicle, followed by invaginations and tissue differentiation, completing development into the adult form (Figure 1A). The source of the germ line in each asexually-derived generation is a population of migratory germ cell precursors, which migrate to new germline niches within the secondary bud at the double vesicle stage ³ (Figure 1A). These germ cell precursors then develop into functional gonads as the primary bud matures into an adult zooid ⁴.

To date, germline stem cell biology has been studied in a limited number of model organisms, and most of our knowledge comes from studies in flies and nematodes, which are phylogenetically very distant from vertebrates. In these species, germ cell fate is specified by a maternally synthesized germ plasm, while in mammals and many other chordates, germ cells form at later stages of development by inductive signals from neighboring tissues ¹. Despite these large phylogenetic distances and differences in the mechanisms of germ cell specification, the genes that are critical for specifying and maintaining germ cell fate are highly conserved across phyla. Examples include *vasa*, *nanos*, *pumilio* and *piwi*, which are not only required for early germ cell specification, but throughout germ line development in most organisms ⁵. *Vasa* encodes an ATP-dependent RNA-helicase, and it is expressed by germ cells and primordial germ cells in most phyla studied to date ^{6,7}. *Vasa* is therefore a reliable marker for primordial germ cells in all animals. Germ cell migration has been studied in flies, zebrafish and mice, and although there are important differences in the underlying mechanisms, several shared principles exist. For example, signaling from G-protein coupled receptors appears to be essential for the directed migration of germ cells. Also, lipid signaling pathways play important roles in germ cell migration in several model organisms (reviewed in ⁸). However, the specific receptors and signaling pathways can differ greatly between species. In *Drosophila*, directional migration of germ cells is guided by signaling from the receptor Tre-1, a G-protein coupled receptor of the rhodopsin family, whereas in zebrafish and mice, CXCR4-signaling mediates the chemotactic response of germ cells. Therefore, in order to gain a deeper understanding of the mechanisms regulating germ cell migration and their evolution, it is essential to study these mechanisms across different phyla. Here, we aim to identify the pathways governing germ cell migration in *Botryllus schlosseri*, an invertebrate chordate.

Sphingosine-1-phosphate (S1P) is a bioactive lipid-signaling molecule that regulates multiple essential cellular processes, including cell growth and survival, as well as cell motility and trafficking. Increased S1P production has been implicated in various pathophysiological processes such as cancer, allergy and autoimmune diseases⁹. Studies in *Drosophila* have suggested a role for phospholipid signaling in regulating germ cell migration and survival¹⁰, but a role of S1P in germ cell migration has not been demonstrated in any species to date. S1P is generated by phosphorylation of sphingosine by sphingosine kinase 1 (Sphk1) at the inner leaflet of the plasma membrane^{9, 11}. This leads to spatially restricted formation of S1P that can be exported out of cells by ABC transporter family members. S1P can then bind to its receptor, S1P receptor type 1 (S1pr1), on the same or neighboring cells to stimulate G-protein regulated signaling pathways. Thus, intracellularly generated S1P can signal “inside-out” through its cell surface receptors in an autocrine or paracrine manner^{9, 11}. S1P levels are tightly regulated by the balance between synthesis by Sphk1, reversible conversion to sphingosine by specific S1P phosphatases (Spp1 and Spp2) and other lipid phosphate phosphatase (Lpp’s), and irreversible degradation by S1P lyase^{9, 11}.

Previous studies have demonstrated that in *Botryllus*, a population of cells enriched for germ cell marker genes and germline stem cell function can be prospectively isolated based on expression of aldehyde dehydrogenases (ALDH)¹², though only 1 out of 50 ALDH-positive cells functionally reconstitutes the germ line of a recipient. Here, we develop a novel method of prospective isolation of a highly enriched population of germ cell precursors, based on expression of ALDH and integrin-alpha-6. We show that integrin alpha-6 (Ia6) and S1pr1 are expressed on migrating *vasa*-positive germ cells, and that ALDH/Ia6-positive cells respond to S1P with increased migratory activity, while inhibition of S1P signaling disrupts homing of *vasa*-positive germ cells *in vivo*. We have identified sphingosine-1-phosphate as a crucial chemoattractant-signaling pathway directing migration of germ cells in an invertebrate chordate.

Results

Vasa-positive germ cells express *integrin-alpha-6* and *s1pr1*

Because of the established roles of sphingosine 1-phosphate in migration of immune cells and hematopoietic stem cells^{11, 13} in humans and mice, we aimed to analyze the expression of sphingosine-1-phosphate receptor genes in germ cells from *Botryllus*. We performed a BLAST search, and found two sphingosine-1-phosphate receptor genes in the *Botryllus* genome, which share sequence homology with the vertebrate genes *s1pr1* (28%, identity, E-value = 1e-30) and *s1pr4* (35% identity, E-value = 0.005).

Integrin-alpha 6 is a marker on the surface of spermatogonial stem cells¹⁴ and embryonic stem cells¹⁵. We performed a BLAST search of non-redundant protein sequences, and found a *Botryllus* homolog of *integrin-alpha-6* (34% identity, E-value = 1e-166).

ALDH-positive cells, which are enriched for germ cells, were isolated by flow cytometry. By quantitative RT-PCR analysis, we found that ALDH-positive cells express high levels of *s1pr1* and *integrin-alpha 6* (Supplementary Fig 1a). *Integrin alpha 6* is expressed at 12.1-

fold higher levels in ALDH-positive cells with respect to ALDH-negative cells, and *s1pr1* is expressed at 6.6-fold higher levels (Supplementary Fig 1a). *S1pr4* was expressed at very low levels (Supplementary Fig 1a). To investigate the expression of *s1pr1* and *integrin alpha 6* in *vasa*-positive germ cells, we performed double labeled whole-mount fluorescent *in situ* hybridization (FISH) for *s1pr1* and *Integrin alpha 6* together with *vasa* (Figure 1b). Double FISH showed that the germ cell specific gene *vasa* is expressed together with *integrin-alpha-6*, and all *vasa*-positive cells were found to be *integrin-alpha 6*-positive (Figure 1b). *S1pr1* expression was detected in almost all *vasa*-positive cells (Figure 1b), and was not detected outside of the germ line.

Integrin-alpha-6 is a surface marker of germ cell precursors

Previous studies showed that in *Botryllus*, germline precursors can be enriched by flow cytometry based on expression of aldehyde dehydrogenase (ALDH), and that ALDH-positive cells functionally reconstituted the germ line of recipients following transplantation, while ALDH-negative cells did not¹². ALDH-positive cells are highly enriched for conserved genes that are known to be important regulators of germ cell fate, and required for germline stem cell (GSC) maintenance^{5, 16}, such as *vasa*, *piwi*, *pumilio*, and *CCR4-NOT complex subunit 6 (cnot6)* (Supplementary Fig 1a). However, only 1 out of 50 cells functionally reconstituted the germ line of a recipient¹². Based on our *in situ* hybridization data (Figure 1b), all *vasa*-positive cells also express *integrin-alpha-6*. The high level of homology between the human and *Botryllus* integrin-alpha-6 at the amino acid level prompted us to attempt to stain *Botryllus* cells for flow cytometry using an anti-human-integrin-alpha-6 antibody. In a suspension of cells from *Botryllus* colonies, ALDH-positive cells comprise between 10-20% of total cells (Figure 2a). Around 6% of total cells are double-positive for ALDH and integrin alpha-6 (Figure 2a). The specificity of the antibody-staining was confirmed using an isotype control. We then isolated both integrin-alpha-6-positive and -negative cells from the ALDH-positive population, and analyzed their gene expression by quantitative RT-PCR (Figure 2a). *Vasa*, *piwi*, *pumilio*, and *cnot6* were significantly enriched in integrin-alpha-6-positive (Ia6+) cells compared to integrin-alpha-6-negative cells (Ia6-), with *vasa*, *piwi* and *cnot6* being expressed at 6 to 7 fold higher levels, and *pumilio* at 3.9 fold higher levels in Ia6-positive cells (Figure 2b). *Integrin-alpha-6*, *integrin beta-1* and *s1pr1* expression were also significantly enriched in Ia6+ cells, with *integrin alpha-6* being expressed at 6.5 fold higher levels and *s1pr1* at 8.5 fold higher levels (Figure 2b). In *Drosophila*, the lipid phosphate phosphatase *wunen* mediates phospholipid uptake and hydrolysis^{8, 10}. It is expressed at high levels in somatic cells, and regulates directional migration and survival of germ cells, probably by establishing a gradient of an unknown phospholipid substrate. *Wunen* expression is also required in germ cells for their migration and survival (reviewed in⁸). The closest mammalian homologs of *wunen* are lipid phosphate phosphatases (Lpp). *Botryllus* has one Lpp homolog, and it is expressed in Ia6+ cells at 5.3 fold higher levels compared to IA6-negative cells (Figure 2b).

Sphingosine-1-phosphate stimulates migration of germ cells

To directly test whether S1P stimulates chemotaxis of *Botryllus* germ cells, we performed a transwell migration assay, in which freshly isolated Ia6+ or Ia6- cells were placed on top of a transwell filter. The numbers of cells migrating to different concentrations of S1P in the

bottom chamber were quantified and normalized to control wells to which no stimulant was added. Only Ia6+ cells responded to S1P with significantly increased migratory activity (t -test $p=0.02$), whereas the migration of Ia6- cells was only slightly stimulated by S1P (Figure 3a). Intriguingly, the migratory response of Ia6+ cells was much higher towards 2 μ M S1P (4.7 fold) than towards 20 μ M S1P (1.8 fold). This is consistent with the concept that cells migrating along a chemotactic gradient will slow their migration once they reach regions with higher concentrations of the chemoattractant, due to receptor desensitization¹⁷. To test whether this migratory response of germ cells towards S1P is mediated by the *Botryllus* homolog of the vertebrate S1pr-1, which is expressed in *vasa*-positive cells (Figure 1b), Ia6+ cells were exposed to S1P in the presence of the specific S1pr-1-antagonist W146. W146 significantly reduced the migration of Ia6+ cells to S1P (t -test $p=0.005$), indicating that this migration depends on signaling through S1pr-1 (Figure 3b). The vertebrate form of the G-protein-coupled S1pr1 activates multiple downstream signaling components, including PI3K and Rac1^{11, 18}. We confirmed that the migratory activity induced by S1P in Ia6+ cells from *Botryllus* also depends on activation of PI3K and Rac1 downstream of S1pr1, as inhibitors of these signaling molecules (Wortmannin and NSC 23766,, respectively) likewise blocked migration to S1P (Figure 3b).

G-protein-coupled chemokine receptors such as S1pr-1 activate integrins, thereby regulating adhesion, cell polarity and motility. Integrins play important roles in germ cell migration, presumably through their interaction with the extracellular matrix^{19, 8}. Ligand binding by integrin heterodimers results in signal transduction events controlling cell motility. The extracellular matrix protein laminin affects cell migration and polarization, and has been implicated in germ cell migration in mice and flies^{20, 8, 21}. The integrin heterodimer alpha-6/beta-1 is an important receptor for laminin in neurons, lymphocytes, macrophages, fibroblasts, platelets and other cell types. ALDH-positive/integrin-alpha-6-positive cells express *integrin-beta-1*, leading us to hypothesize that in *Botryllus*, germ cell migration may, at least in part, be mediated by binding to laminin. Laminin alone significantly (t -test $p=0.05$) increased the migratory activity of Ia6+ cells, and the migratory response to S1P was significantly (t -test $p=0.05$) increased on laminin compared to uncoated plastic (Figure 3c). On laminin, the migratory response to S1P was completely inhibited by an integrin-alpha-6-blocking antibody, whereas migration on plastic was unaffected by this antibody (Figure 3c). These results indicate that integrin-alpha-6 is indeed part of a laminin receptor, and that S1pr-1 regulates chemotaxis to S1P by activating Integrin alpha 6.

***In vivo* expression of *s1pr1* on migrating germ cells**

To characterize the migratory paths of *Botryllus* germ cells *in vivo*, and in particular during the formation of secondary buds, we performed whole-mount fluorescent *in situ* hybridization (FISH) for *vasa* and *s1pr1* on colonies in all stages of secondary bud formation. By FISH, *s1pr1* and *vasa* are expressed in small, round cells (7-10 μ m in diameter) with the high nuclear to cytoplasmic ratio characteristic of primordial germ cells and germline stem cells (GSC) (Figure 4). These cells are present in the peripheral blood vessels, particularly in vascular protrusions known as ampullae, as depicted in the schematic shown in Figure 4a. We hypothesize that these cells enter into the primary bud from the peripheral blood vessels via an unknown path (Figure 4a). Figure 4b and e show FISH

images of ampullae containing round, small cells expressing *vasa*, and *s1pr1*, respectively. As shown in the schematic in figure 4a, on either side of the developing body, and situated adjacent to and proximal to the newly forming secondary buds, slightly larger germ cell precursors (15-30 μm) are present in addition to those small GSC (Figure 4 c and f, arrowheads, and schematic in Figure 4a). These precursors also express *vasa* and *s1pr1*. As the newly forming secondary bud closes and forms a double vesicle, as shown in the schematic in Figure 4a, *vasa* and *s1pr1* positive germ cell precursors migrate into the secondary bud (Figure 4 d and g, arrowheads).

***In vivo* inhibition of S1P signaling blocks germ cell homing**

To test whether S1P regulates homing of germ cell precursors and GSC *in vivo*, animals were treated with small molecule inhibitors of sphingosine-kinase (Sphk1) or an antagonist of S1pr1 (W146). Treatment was started at the stage when the formation of a new secondary bud is in its earliest stage (A1), and barely visible as a thickening of the peribranchial epithelium (Figure 1a, and Figure 4a left). When the secondary bud reached the double vesicle stage, the localization of germ cells was analyzed by FISH for *vasa*. In control animals (untreated), a cluster of *vasa*-positive cells is clearly visible inside the double vesicle stage secondary bud (Figure 5a-c, arrows). In animals treated with inhibitors of Sphk1 or S1pr1-antagonist, double vesicle stage secondary buds contain almost no *vasa*-positive germ cells (Figure 5 e-g, i-k, m-o). The number of secondary buds containing any *vasa*-positive cells was significantly reduced in animals treated with Sphk1-inhibitors (Sphk1-inhibitor A *t*-test $p=0.004$, Sphk1 inhibitor B *t*-test $p=0.01$) or S1pr1-antagonist, (*t*-test $p=0.03$) (Figure 5m). The absence of *vasa*-positive cells in secondary buds of inhibitor treated animals could be due to disrupted homing or lack of engraftment and survival in the secondary bud niche, or both. In animals treated with Sphk1-inhibitors or S1pr1-antagonist (W146), *vasa*-positive germ cell precursors were visible in unusual locations inside the primary bud, such as near the endostyle (Figure 5 e, arrows), which indicates that these cells might be migrating randomly due to inhibition of the homing signal. In addition to the small *vasa*-positive GSC that are present in the blood vessels of untreated control animals (Figure 5a), larger (20-40 μm) *vasa*-positive germ cell precursors were detected inside blood vessels (Figure 5 a and c, arrows) of animals treated with Sphk1-inhibitors or S1pr1-antagonist W146. Compared to control animals, the number of large *vasa*-positive precursors present in the vasculature was significantly increased in drug treated animals (Figure 6b). These results demonstrate that in the absence of S1P signaling, germ cell precursors migrate randomly and are not able to home to the secondary buds.

S1P is generated in the germ cell niche

The formation of extracellular gradients of S1P depends on the organization of cell types with varying S1P metabolism²². Some cell types are specialized metabolically to produce high extracellular levels of S1P, while other cell types are metabolically geared toward keeping the extracellular S1P levels low²². To assess the mechanism that results in the formation of different amounts of S1P within the double vesicle stage secondary buds and somatic tissues outside of the secondary bud, we analyzed the expression pattern of *sphingosine-kinase (sphk1)*. By FISH, *sphk1* expression was detected in developing secondary buds at the time when germ cells migrate, at the double vesicle stage (Figure 7a).

LPPs have been implicated in being the major factor contributing to the formation of changes in S1P levels, since other S1P degrading factors, such as S1P-phosphatase and S1P-lyase, are intracellular enzymes and involved in intracellular metabolism of S1P²². In contrast to *sphk1*, *lpp* expression was detected in somatic tissues of the entire primary bud (Figure 7a, but was absent from the germ cell niche. By FISH, *lpp* expression was not detected in germ cells, even though some expression of *lpp* was detected in ALDH/integrin-alpha-6 positive cells by quantitative RT-PCR (Figure 2b), indicating that expression levels of *lpp* in germ cells are below the limit of detection by FISH.

To functionally assess the role of LPP in formation of an S1P gradient, we injected Fluorescein labeled S1P into the blood stream of colonies at the double vesicle stage. Fluorescein-S1P diffuses rapidly into the blood vessels and tissues surrounding the injection site (Figure 7b). After 10 minutes, the FITC label begins to accumulate in developing testes (t), oocytes (o) and the stomach (s) of the primary bud, and this accumulation becomes stronger after 15 minutes, indicating active uptake of the Fluorescein-label in those tissues (Figure 7b). These results are in line with reports that dephosphorylation of S1P by Lpp seems to be necessary for uptake of the resulting sphingosine by cells (reviewed in²²). In fact, sphingosine-Fluorescein injection resulted in the same pattern of accumulation of fluorescence as S1P-Fluorescein (supplementary figure 1c), suggesting that dephosphorylation of S1P-Fluorescein by Lpp leads to uptake of the resulting sphingosine-Fluorescein by developing gonads and the stomach. To confirm this hypothesis, we injected S1P-Fluorescein together with the phosphatase inhibitor sodium-orthovanadate (SOV), which inhibits activity of Lpp⁽²³⁾. In the presence of SOV, no accumulation of fluorescence was detected, and the injected S1P-Fluorescein diffuses rapidly (Figure 7b).

As summarized in Figure 7c, our results show that in *Botryllus*, migration and homing of germ cells to newly developing niches depends on signaling of S1P through S1pr1. S1P is generated by Sphk1 in the developing germ cell niche inside the secondary bud. Dephosphorylation and clearance of S1P appear to be mediated by Lpp expression in somatic tissues of the primary bud.

Discussion

In the present study, we identified a novel role for the phospholipid S1P and the G-protein coupled receptor S1pr1 in chemotactic migration of germ cells. In addition, we have shown that S1P/S1pr1 induced migration of germ cells depends on integrin-alpha-6-mediated binding to laminin, and that integrin-alpha-6 is a marker for germ cell precursors in *Botryllus*. When S1P signaling is disrupted, germ cell precursors migrate randomly and are not able to home to the secondary buds. S1P is generated by Sphk1, which is, expressed in developing germ cell niches, while Lpp mediates dephosphorylation and clearance of S1P in somatic tissues outside of the germ cell niche.

We have demonstrated that in *Botryllus*, an invertebrate chordate, S1P activates a homolog of the vertebrate S1pr1, inducing chemotactic migration of germ cells. This migratory response is dependent on activation of PI3K and Rac1 downstream of the S1P receptor 1, and, ultimately, activation of integrin alpha 6. G-protein coupled receptors mediate cellular

responses to attractive chemokines in a variety of cell types, including germ cells. Tre-1 is a G-protein coupled receptor of the rhodopsin family, and is important for the migration of primordial germ cells across the posterior midgut in *Drosophila*^{8,25}. In mice and zebrafish, primordial germ cells express CXCR4, which controls migration to SDF-1 expressed by somatic cells of the developing gonads⁸. The G-protein-coupled S1PR in *Botryllus* is a novel example of this common theme of germ cell chemotaxis, with a previously unknown role in germ cell migration. A role of S1P in germ cell migration has never been shown previously. SphK1/SphK2 double-knockout mice or S1PR1-knockout mice are not viable^{26,27}, and the role of S1P signaling in germ cell migration in mammals has not been studied to date, but S1P signaling has been well studied for its role in leukocyte migration¹¹. PGC migration most closely resembles amoeboid migration and the migration of immune cells, which is characterized by individually migrating cells with a broad leading edge, highly dynamic morphology and low adhesiveness⁸.

Lipid signaling pathways are a common theme in the process of germ cell migration that is shared among several species in different phyla (reviewed in⁸). In *Drosophila*, the lipid phosphate phosphatases WUN and WUN2, the fly homologs of mammalian LPP's, are expressed in somatic cells, where they repel migrating germ cells¹⁰. WUN and WUN2 function by hydrolysing phospholipids and have also been shown to promote the uptake of dephosphorylated lipids. Thus, wunen activity creates a gradient of an unknown phospholipid substrate, which regulates chemotactic migration of germ cells^{8,28}. Our data demonstrate that a similar mechanism exists in *Botryllus*, where Lpp is involved in degradation of the phospholipid S1P, which regulates migration of germ cells. This suggests a high degree of evolutionary conservation of this mechanism, as tunicates and flies are phylogenetically very distant from each other. Based on our findings in *Botryllus*, it would be interesting to test the role of S1P in germ cell migration in *Drosophila*.

In our study, *lpp* expression was detected on Integrin-alpha-6-positive cells by qPCR, but the levels of expression were too low to be detected by FISH (Figures 2b and 7a). A possible explanation for this is that *lpp* expression might be required for signal termination at the S1P-receptor. S1PR receptor desensitization can occur by receptor internalization²⁹, but Pyne et al¹⁸ proposed an interesting mechanism that involves the dephosphorylation of S1P to sphingosine by LPP1, which is located at the plasma membrane, with an externally oriented catalytic site. Thus, LPP1 may decrease extracellular S1P levels to limit its bioavailability at S1P-receptors. This might require a coordinated mechanism that enables S1P to induce downstream signaling responses before LPP1 is activated to reduce the extracellular concentration of S1P. This could involve an intracellular phosphorylation / dephosphorylation mechanism at cytoplasmic-facing phosphorylation sites of LPP. This mechanism may explain *lpp*-expression on *Botryllus* germ cells (Figure 2b) and wunen expression on migrating germ cells in *Drosophila*. We will test this possibility in future studies.

In our study, disruption of S1P signaling leads to random migration of germ cells. Therefore, it is likely that other pathways exist that stimulate this random migratory activity of *Botryllus* germ cells. In other animal models, receptor tyrosine kinases often provide such signals, whereas chemoattractants signaling through G-protein coupled receptors provide

directional cues. An example of this is PGC migration in mice, where SDF1 and CXCR4 control directional migration, and c-kit is required for motility³⁰. In future experiments, we will test for the role receptor tyrosine kinases in *Botryllus* germ cell migration.

In conclusion, our data show that germ cells in *Botryllus* express a homolog of the vertebrate G-protein coupled receptor S1PR1, and that sphingosine-1-phosphate acts as a chemoattractant, directing the homing of germ cells to niches in newly formed asexual progeny. This is the first description of a role of S1P signaling in germ cell chemotaxis.

Materials and Methods

Animals

Botryllus schlosseri colonies used in this study were lab-cultivated strains, spawned from animals collected in Santa Barbara, CA, and cultured in laboratory conditions at 18-20 °C according to³¹. Animals are reared in 5 L tanks supplemented with food in suspension daily, and food is not limiting. Collections were performed at only one local harbor, the Santa Barbara Harbor (Longitude -119.6887448 and Latitude 34.407), which is owned by the City of Santa Barbara and performed under the authority of the California Department of Fish and Game. These collections did not involve any endangered or protected species. Colonies were developmentally staged according to².

Cell Sorting

Genetically identical, stage matched animals were pooled, and a single cell suspension was generated by mechanical dissociation. Whole animals were minced and passed through 70 µm and 40 µm cell strainers in ice-cold sorting buffer (filtered sea-water with 2% horse serum and 50mM EDTA). Aldefluor dye (Stem Cell Technologies) was added to cell suspensions at 1/100 dilution, together with Anti-Human/Mouse-CD49f-eFluor450 (Ebioscience, cloneGoH3, 1/100 dilution) and incubated on ice for 30 min and washed with sorting buffer. Fluorescence activated cell sorting (FACS) was performed using a FACSAria (BD Biosciences) cell sorter. Samples were gated as ALDH-positive or -negative based on unstained control fluorescence, and as CD49f-positive or -negative based on isotype control staining (RatIgG2A-isotype-control eFluor450, Ebioscience). Analysis was performed using FACSDiva software (BD Biosciences). Cells were sorted using a 70 µm nozzle and collected into sorting buffer.

Quantitative RT PCR

Sorted cells were pelleted at 700g for 10min, and RNA was extracted using the Nucleospin RNA XS kit (Macherey Nagel), which included a DNase treatment step. RNA was reverse transcribed into cDNA using random primers (Life Technologies) and Superscript II Reverse Transcriptase (Life Technologies). Quantitative RT-PCR (Q-PCR) was performed using a LightCycler 480 II (Roche) and LightCycler DNA Master SYBR Green I detection (Roche) according to the manufacturer's instructions. The thermocycling profile was 5 min at 95, followed by 45 cycles of 95 °C for 10 sec, 60 °C for 10 sec. The specificity of each primer pair was determined by BLAST analysis (to human, *Ciona* and *Botryllus* genomes), by melting curve analysis and gel electrophoresis of the PCR product. To control for

amplification of genomic DNA, 'no RT'-controls were used. Primer pairs were analyzed for amplification efficiency using calibration dilution curves. All genes included in the analysis had CT values of <35. Primer sequences are listed in Supplementary Table 1. Relative gene expression analysis was performed using the 2^{-CT} Method. The CT of the target gene was normalized to the CT of the reference gene *elongation factor 1 alpha* (EF1a): $CT = CT_{(target)} - CT_{(EF1a)}$. To calculate the normalized expression ratio, the CT of the test sample (IA6-positive cells) was first normalized to the CT of the calibrator sample (IA6-negative cells): $CT = CT_{(IA6-positive)} - CT_{(IA6-negative)}$. Second, the expression ratio was calculated: $2^{-CT} = \text{Normalized expression ratio}$. The result obtained is the fold increase (or decrease) of the target gene in the test samples relative to IA6-negative cells. Each qPCR was performed at least three times on cells from independent sorting experiments gene was analyzed in duplicate in each run. The CT between the target gene and EF1alpha was first calculated for each replicate and then averaged across replicates. The average CT for each target gene was then used to calculate the CT as described above. Data are expressed as averages of the normalized expression ratio (fold change). Standard deviations were calculated for each average normalized expression ratio. Statistical analysis was performed using a paired, two-sided Student's *t*-test. ** = $p < 0.05$

***In Situ* Hybridization**

Whole mount *in situ* hybridization was performed as described in ³². Briefly, *B. schlosseri* homologs of genes of interest were identified by blastn searches of the *B. schlosseri* EST database (http://octopus.obs-vlfr.fr/public/botryllus/blast_botryllus.php) using human or Ciona (when available) protein sequences. Primer pairs were designed to amplify a 500-800 bp fragment of each transcript (Primer sequences in Supplementary table 1). PCR was performed with Advantage cDNA Polymerase (Clontech, 639105) and products were cloned into the pGEM-T Easy vector (Promega, A1360). Cloned fragments were sequenced and analyzed by Blastx to ensure that the correct sequence was cloned. *In vitro* transcription of antisense probes was performed with SP6 or T7 RNA polymerase (Roche, 10810274001, 10881767001) using either digoxigenin or dinitrophenol labeling. *B. schlosseri* were anesthetized with 0.02% Tricaine (TCI, T0941) in seawater for 10 min, and then fixed with 4% formaldehyde in 0.5 M NaCl, for 3h at room temperature. Fixed samples were then dehydrated with methanol and bleached overnight in 6% H₂O₂ in methanol under direct light. Samples were rehydrated stepwise into PBST and permeabilized by treatment with 10 mg/ml proteinase K (Roche, 03115879001) in PBST for 30 minutes at room temperature. A post-fixation step was performed with 4% formaldehyde in PBST for 20 min at room temperature. Samples were then washed with PBST and incubated in hybridization buffer (65% formamide, 5× SSC, 1× Denhardt's solution, 0.1% Tween-20, 5 mg/ml torula yeast RNA, 50 mg/ml heparin) without probe for 4–6 h at 58–65°C, followed by overnight incubation with digoxigenin-labeled riboprobes diluted in hybridization buffer at 58–65°C. Control samples were incubated with sense probes. Following hybridization, unbound probes were washed away by a series of low-salt washes and samples were incubated in blocking solution (PBST, 5% heat-inactivated horse serum, 2 mg/ml bovine serum albumin) for 4 h at room temperature. Probes were detected using HRP-conjugated anti-digoxigenin antibody (Roche, 11207733910) at a dilution of 1/1000 or HRP-conjugated anti-dinitrophenol antibody (Perkin Elmer, FP1129) at a dilution of 1/200. After incubation with

antibody, the samples were washed extensively in PBST + 2 mg/ml bovine serum albumin and transferred to PBS. Digoxigenin-labeled probes were then detected by fluorophore deposition using the TSA Plus System (Perkin Elmer, NEL753001KT). Nuclei were stained with Hoechst 33342 (Life Technologies). Imaging of labeled samples was performed using an Olympus FLV1000S Spectral Laser Scanning Confocal.

Transwell Migration Assay

Transwell filters with 8µm pore size inserted in a 24 well plate (Corning) were coated with laminin over night at 4°C and briefly air dried before adding 50,000 sorted cells, resuspended in 100µl filtered seawater with 10% DMEM and 1% FBS. The bottom of the well contained filtered seawater with 10% DMEM /1% FBS. Sphingosine-1-phosphate (0.2 - 20µM), 10µM S1PR-1-inhibitor W146, 0.1µM PI3K-inhibitor Wortmannin, 100µM Rac1-inhibitor NSC 23766 (all from Tocris), 5µg/ml anti-Integrin-alpha-6 (clone GoH3, Ebioscience) or isotype control antibody were added to the bottom chamber where applicable. After 2 hours incubation at room temperature, nuclei were stained with Hoechst 33342 and counted in images taken at 3 random locations of the bottom well (at 100× magnification) using the “cell counter” plugin in FIJI software. All assays were performed in triplicates with cells from 3 independent sorts. Statistical analysis was performed using a paired, two-sided Student’s *t*-test.

Small Molecule Inhibitor Treatment

Animals were incubated in 30 ml of sea water containing 1µM Sphingosine-Kinase-Inhibitor (A) SKI-I (Abcam), 14µM Sphingosine-Kinase-Inhibitor (B) CAS 1177741-83-1 (Millipore 567731), or 10 µM S1PR1 antagonist W146 (Tocris). Seawater containing drugs was replaced and fresh food (algae) was added daily. Controls were incubated in sea water without inhibitors with vehicle ethanol 0.1% or DMSO 0.001%. After 4 days, animals were fixed and analyzed by *in situ* hybridization as described above. For each treatment, two genetically identical colonies were treated simultaneously, and the experiment was performed three times. Buds containing *vasa*-positive cells and the number of *vasa*-positive cells in the vasculature were counted on each treated and untreated colony under an epifluorescence microscope. Data are expressed as averages from three experiments, and statistical analysis was performed using a paired, two-sided Student’s *t*-test.

S1P-Fluorescein live imaging

Colonies were microinjected into the blood stream with 1µl of 0.1mg/ml S1P-Fluorescein in sea water, with or without 10mM sodium-orthovanadate. Colonies were placed under sea water on top of an inverted epifluorescence microscope (Olympus) equipped with a cooled camera. Images of green fluorescence were taken at 2 minutes after injection, and every 5 minutes thereafter.

Supplementary Material

Refer to Web version on PubMed Central for supplementary material.

Acknowledgements

The authors would like to thank Mike Caun for expert animal care, as well as Brian Braden and Alessandro Di Maio for helpful discussions and advice. We also thank Mary Raven and the UCSB microscopy facility. SHK was supported by a postdoctoral fellowship from the California Institute of Regenerative Medicine. This work was funded by NIH grants AG037966 and DK045762.

References

1. Saffman EE, Lasko P. Germline development in vertebrates and invertebrates. *Cell Mol Life Sci.* 1999; 55:1141–1163. [PubMed: 10442094]
2. Lauzon RJ, Ishizuka KJ, Weissman IL. Cyclical generation and degeneration of organs in a colonial urochordate involves crosstalk between old and new: a model for development and regeneration. *Developmental biology.* 2002; 249:333–348. [PubMed: 12221010]
3. Brown FD, et al. Early lineage specification of long-lived germline precursors in the colonial ascidian *Botryllus schlosseri*. *Development.* 2009; 136:3485–3494. [PubMed: 19783737]
4. Rodriguez D, et al. Analysis of the basal chordate *Botryllus schlosseri* reveals a set of genes associated with fertility. *BMC Genomics.* 2014; 15:1183. [PubMed: 25542255]
5. Lehmann R. Germline stem cells: origin and destiny. *Cell Stem Cell.* 10:729–739. [PubMed: 22704513]
6. Mochizuki K, Nishimiya-Fujisawa C, Fujisawa T. Universal occurrence of the vasa-related genes among metazoans and their germline expression in *Hydra*. *Dev Genes Evol.* 2001; 211:299–308. [PubMed: 11466525]
7. Extavour CG, Akam M. Mechanisms of germ cell specification across the metazoans: epigenesis and preformation. *Development.* 2003; 130:5869–5884. [PubMed: 14597570]
8. Richardson BE, Lehmann R. Mechanisms guiding primordial germ cell migration: strategies from different organisms. *Nat Rev Mol Cell Biol.* 2010; 11:37–49. [PubMed: 20027186]
9. Kim RH, Takabe K, Milstien S, Spiegel S. Export and functions of sphingosine-1-phosphate. *Biochim Biophys Acta.* 2009; 1791:692–696. [PubMed: 19268560]
10. Renault AD, Sigal YJ, Morris AJ, Lehmann R. Soma-germ line competition for lipid phosphate uptake regulates germ cell migration and survival. *Science.* 2004; 305:1963–1966. [PubMed: 15331773]
11. Rosen H, Goetzl EJ. Sphingosine 1-phosphate and its receptors: an autocrine and paracrine network. *Nat Rev Immunol.* 2005; 5:560–570. [PubMed: 15999095]
12. Laird DJ, De Tomaso AW, Weissman IL. Stem cells are units of natural selection in a colonial ascidian. *Cell.* 2005; 123:1351–1360. [PubMed: 16377573]
13. Mierzejewska K, et al. Sphingosine-1-phosphate-mediated mobilization of hematopoietic stem/progenitor cells during intravascular hemolysis requires attenuation of SDF-1-CXCR4 retention signaling in bone marrow. *Biomed Res Int.* 2013; 2013:814549. [PubMed: 24490172]
14. Shinohara T, Avarbock MR, Brinster RL. beta1- and alpha6-integrin are surface markers on mouse spermatogonial stem cells. *Proc Natl Acad Sci U S A.* 1999; 96:5504–5509. [PubMed: 10318913]
15. Cooper HM, Tamura RN, Quaranta V. The major laminin receptor of mouse embryonic stem cells is a novel isoform of the alpha 6 beta 1 integrin. *J Cell Biol.* 1991; 115:843–850. [PubMed: 1833411]
16. Joly W, Chartier A, Rojas-Rios P, Busseau I, Simonelig M. The CCR4 deadenylase acts with Nanos and Pumilio in the fine-tuning of Mei-P26 expression to promote germline stem cell self-renewal. *Stem Cell Reports.* 2013; 1:411–424. [PubMed: 24286029]
17. Wu D, Lin F. Modeling cell gradient sensing and migration in competing chemoattractant fields. *PLoS One.* 2011; 6:e18805. [PubMed: 21559528]
18. Pyne S, Pyne NJ. Sphingosine 1-phosphate signalling in mammalian cells. *Biochem J.* 2000; 349:385–402. [PubMed: 10880336]
19. Anderson R, et al. Mouse primordial germ cells lacking beta1 integrins enter the germline but fail to migrate normally to the gonads. *Development.* 1999; 126:1655–1664. [PubMed: 10079228]

20. Garcia-Castro MI, Anderson R, Heasman J, Wylie C. Interactions between germ cells and extracellular matrix glycoproteins during migration and gonad assembly in the mouse embryo. *J Cell Biol.* 1997; 138:471–480. [PubMed: 9230086]
21. Jaglarz MK, Howard KR. The active migration of *Drosophila* primordial germ cells. *Development.* 1995; 121:3495–3503. [PubMed: 8582264]
22. Olivera A, Allende ML, Proia RL. Shaping the landscape: metabolic regulation of S1P gradients. *Biochim Biophys Acta.* 2013; 1831:193–202. [PubMed: 22735358]
23. Peest U, et al. S1P-lyase independent clearance of extracellular sphingosine 1-phosphate after dephosphorylation and cellular uptake. *J Cell Biochem.* 2008; 104:756–772. [PubMed: 18172856]
24. O’Sullivan C, Dev KK. The structure and function of the S1P1 receptor. *Trends Pharmacol Sci.* 2013; 34:401–412. [PubMed: 23763867]
25. Santos AC, Lehmann R. Germ cell specification and migration in *Drosophila* and beyond. *Curr Biol.* 2004; 14:R578–589. [PubMed: 15268881]
26. Mizugishi K, et al. Essential role for sphingosine kinases in neural and vascular development. *Mol Cell Biol.* 2005; 25:11113–11121. [PubMed: 16314531]
27. Gaengel K, et al. The sphingosine-1-phosphate receptor S1PR1 restricts sprouting angiogenesis by regulating the interplay between VE-cadherin and VEGFR2. *Dev Cell.* 2012; 23:587–599. [PubMed: 22975327]
28. Santos AC, Lehmann R. Isoprenoids control germ cell migration downstream of HMGCoA reductase. *Dev Cell.* 2004; 6:283–293. [PubMed: 14960281]
29. Thangada S, et al. Cell-surface residence of sphingosine 1-phosphate receptor 1 on lymphocytes determines lymphocyte egress kinetics. *J Exp Med.* 2010; 207:1475–1483. [PubMed: 20584883]
30. Gu Y, Runyan C, Shoemaker A, Surani A, Wylie C. Steel factor controls primordial germ cell survival and motility from the time of their specification in the allantois, and provides a continuous niche throughout their migration. *Development.* 2009; 136:1295–1303. [PubMed: 19279135]
31. Boyd HC, Harp JA, Weissman IL. Growth and sexual maturation of laboratory-cultured Monterey *Botryllus schlosseri*. *Biological Bulletin.* 1986; 170:91–109. B.S.
32. Langenbacher AD, Rodriguez D, Di Maio A, De Tomaso AW. Whole-mount fluorescent in situ hybridization staining of the colonial tunicate *Botryllus schlosseri*. *Genesis.* 2015; 53:194–201. [PubMed: 25179474]

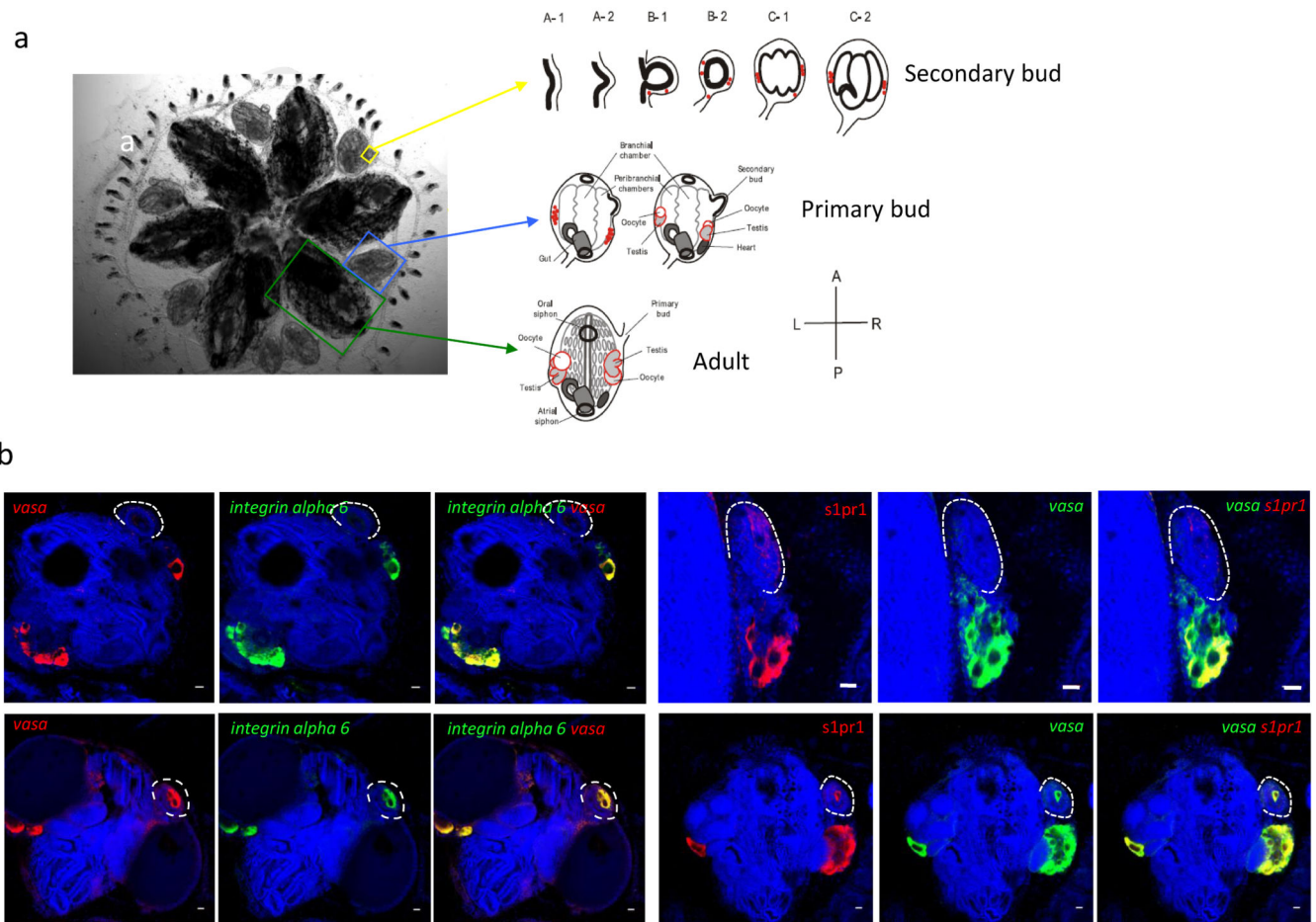


Figure 1. *Botryllus Schlosseri* morphology, gonad formation and expression of *integrin-alpha-6* and *s1pr1* in *vasa*-positive cells

a) ventral view of a colony of individual adult animals (green boxes and arrows), each of which is connected to asexual propagating primary buds (blue boxes and arrows) and secondary buds (yellow boxes and arrows). During the asexual budding process, new buds form as a thickening of the peribranchial epithelium (stage A), which forms a pocket and eventually closes to form a double vesicle (stage B). Buds undergo invaginations and differentiate into all somatic tissues and organs (stage C). Germ cells (red) enter the newly formed secondary buds at stage B, and differentiate into testes and oocytes, as primary buds develop into the adult form. Individual animals are connected by a common extracorporeal vasculature, which ends in terminal projections known as ampullae (a). **b)** Representative examples of expression patterns of *integrin-alpha-6* and *s1pr1* in *vasa*-positive by double-labeled fluorescent in situ hybridization (n=5). Left panel: All *vasa*-positive (red) germ cell precursors co-express *integrin-alpha-6* (green). Right panel: *S1pr1* (red) is expressed in *vasa*-positive cells (green). Red and green channels are shown individually together with nuclear counterstaining (blue), and merged images show co-expression of both genes (yellow). Top panels represent stages prior to homing of *vasa*-positive cells into the secondary buds. Note that the weak red signal on the secondary bud at this stage is due to slight trapping of the probe inside the secondary bud, and not true signal for *s1pr1* mRNA.

Bottom panels represent stages after homing of vasa-positive cells into the secondary buds. Nuclei were counterstained with Hoechst 33342 (blue). For better orientation, secondary buds have been outlined with broken white lines. Scale bars = 20 μ m.

Author Manuscript

Author Manuscript

Author Manuscript

Author Manuscript

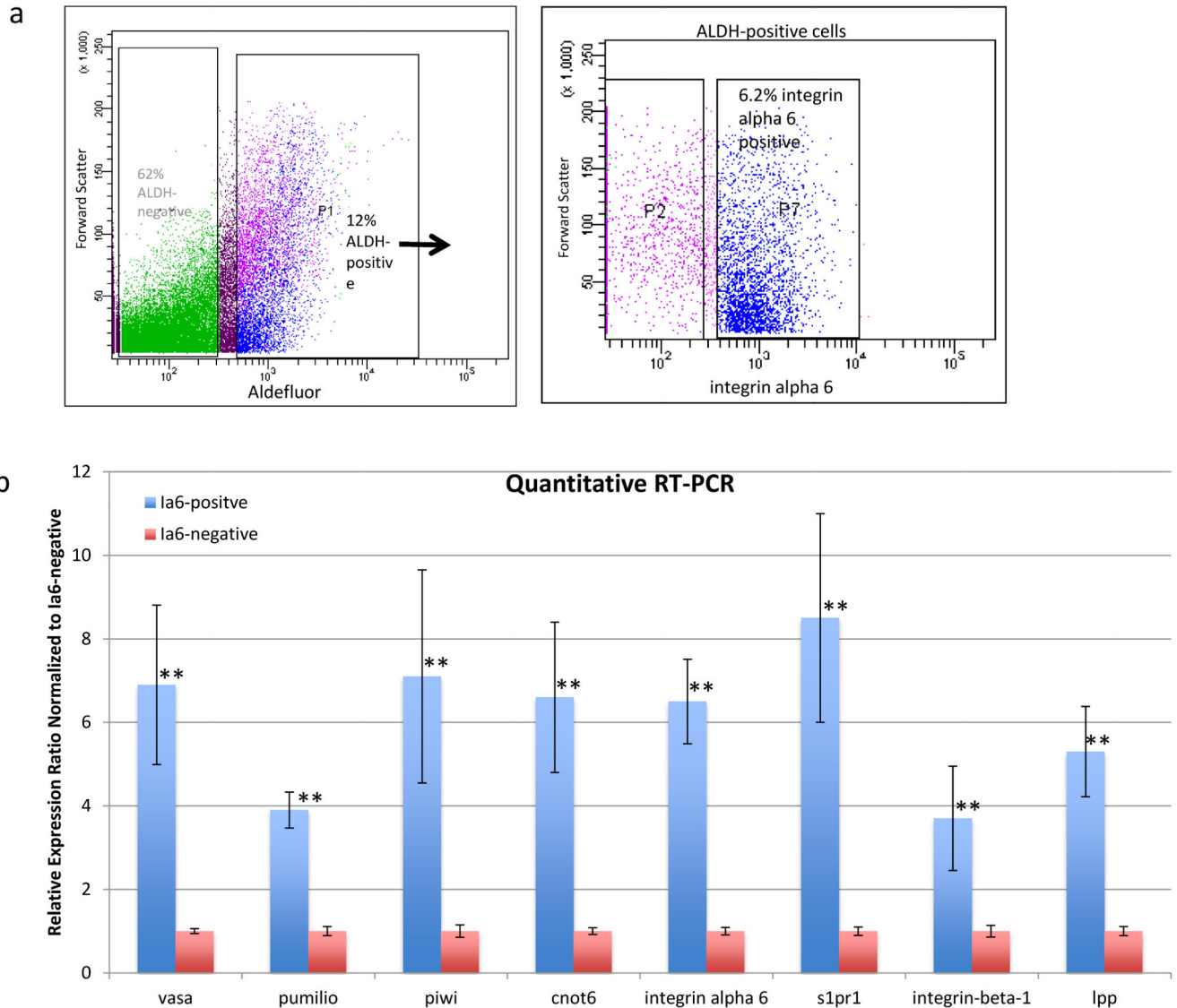


Figure 2. Prospective isolation of germ cell precursors based on expression of aldehyde dehydrogenase and Integrin-alpha-6, gene expression analysis

a) Representative example of fluorescence-activated-cell-sorting (n=20). Aldehyde dehydrogenase (ALDH)-positive and -negative cells were gated based on Aldefluor-fluorescence compared to unstained controls, and 12% of total cells are ALDH-positive. From the ALDH-positive-population (arrow), Integrin-alpha-6-positive (p7) and -negative cells (p2) were gated based on isotype control staining. 6.2% of total cells are ALDH-positive/Integrin-alpha-6-positive.

b) Q-RT-PCR analysis of Integrin-alpha-6 (Ia6)-positive or -negative cells sorted from the ALDH-positive population. Relative quantification was performed using the 2^{-CT} -method, with *ef1a* as control gene. Data are expressed as averages of the relative expression ratio (fold change), normalized to Ia6-negative cells. Standard deviations were calculated for each average expression ratio (n=3). Statistical analysis was performed using Student's *t*-test. ** indicates $p < 0.05$ (medium significance compared to Ia6-negative cells).

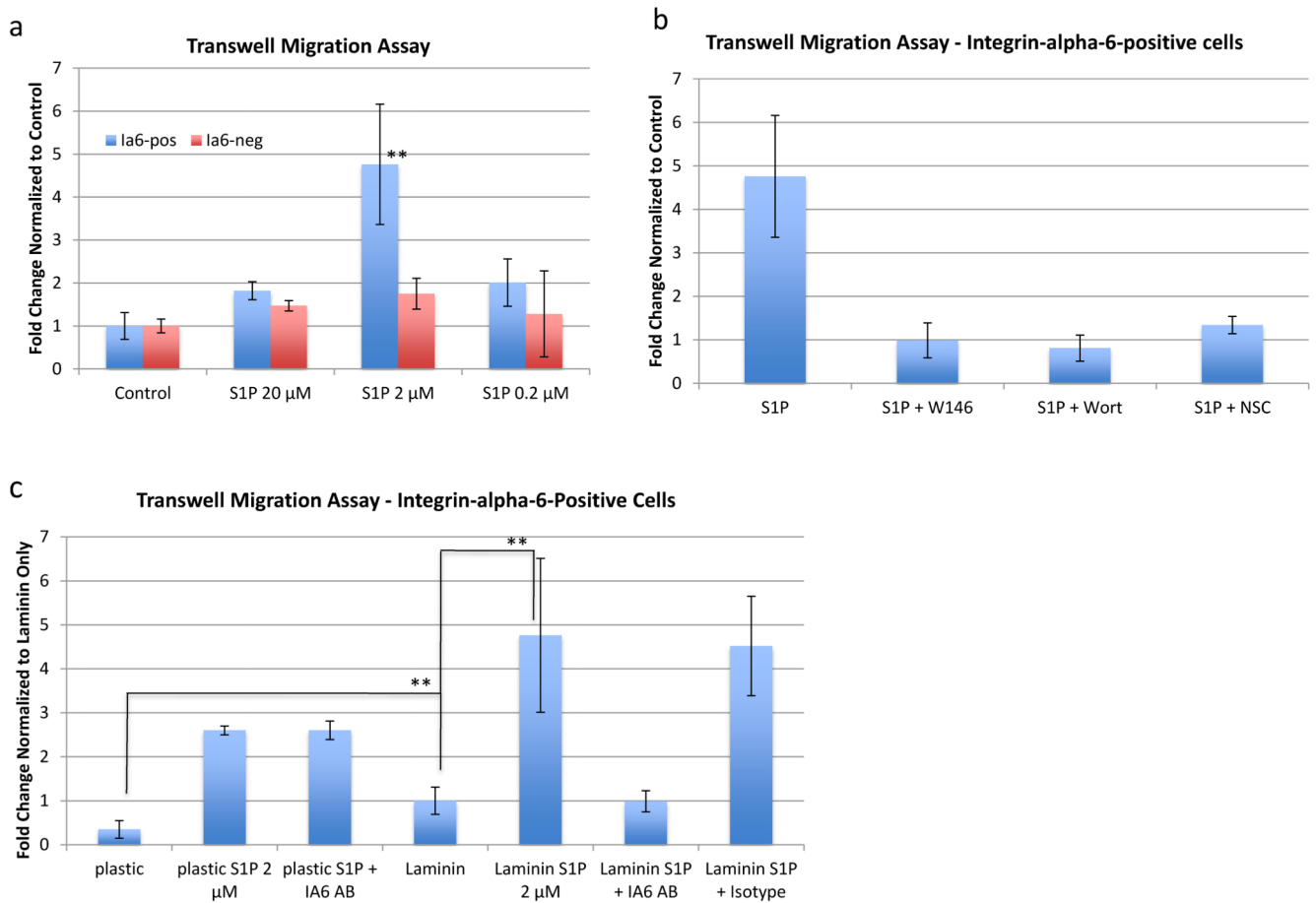


Figure 3. The migration of Integrin-alpha-6-positive germ cell precursors towards sphingosine-1-phosphate is mediated by the G-protein coupled receptor S1PR1 and Integrin-alpha-dependent binding to laminin

a) Migration assay of ALDH-positive cells in response to different concentrations of S1P, as indicated. No stimulant was added to control wells. Sorted cells were added to the upper chamber of a transwell system coated with laminin, and after 2 h, migrated cells in the lower chamber were counted. Data are expressed as fold changes of numbers of migrated cells, normalized to unstimulated controls (n=6). Statistical analysis was performed using Student's *t*-test. ** indicates $p < 0.05$ (medium significance compared to control). **b)** Migration assay of ALDH-positive/Integrin-alpha-6-positive cells in the presence of 2 μ M S1P with or without inhibitors of S1PR signaling. S1PR1 antagonist W146 (10 μ M), PI3K-inhibitor Wortmannin (0.1 μ M) or Rac1-inhibitor NSC (100 μ M) were added as indicated. Data are expressed as fold changes of numbers of migrated cells, normalized to unstimulated controls. **c)** Migration assay of ALDH-positive/Integrin-alpha-6-positive cells on uncoated plastic or laminin coated transwells with or without 2 μ M S1P. Anti-Integrin-alpha-6 (5 μ g/ml) or isotype control antibody was added as indicated. Data are expressed as fold changes of numbers of migrated cells, normalized to unstimulated controls on laminin. Error bars represent the standard deviation for each average (n=6). Statistical analysis was performed using Student's *t*-test. ** indicates $p < 0.05$ (medium significance).

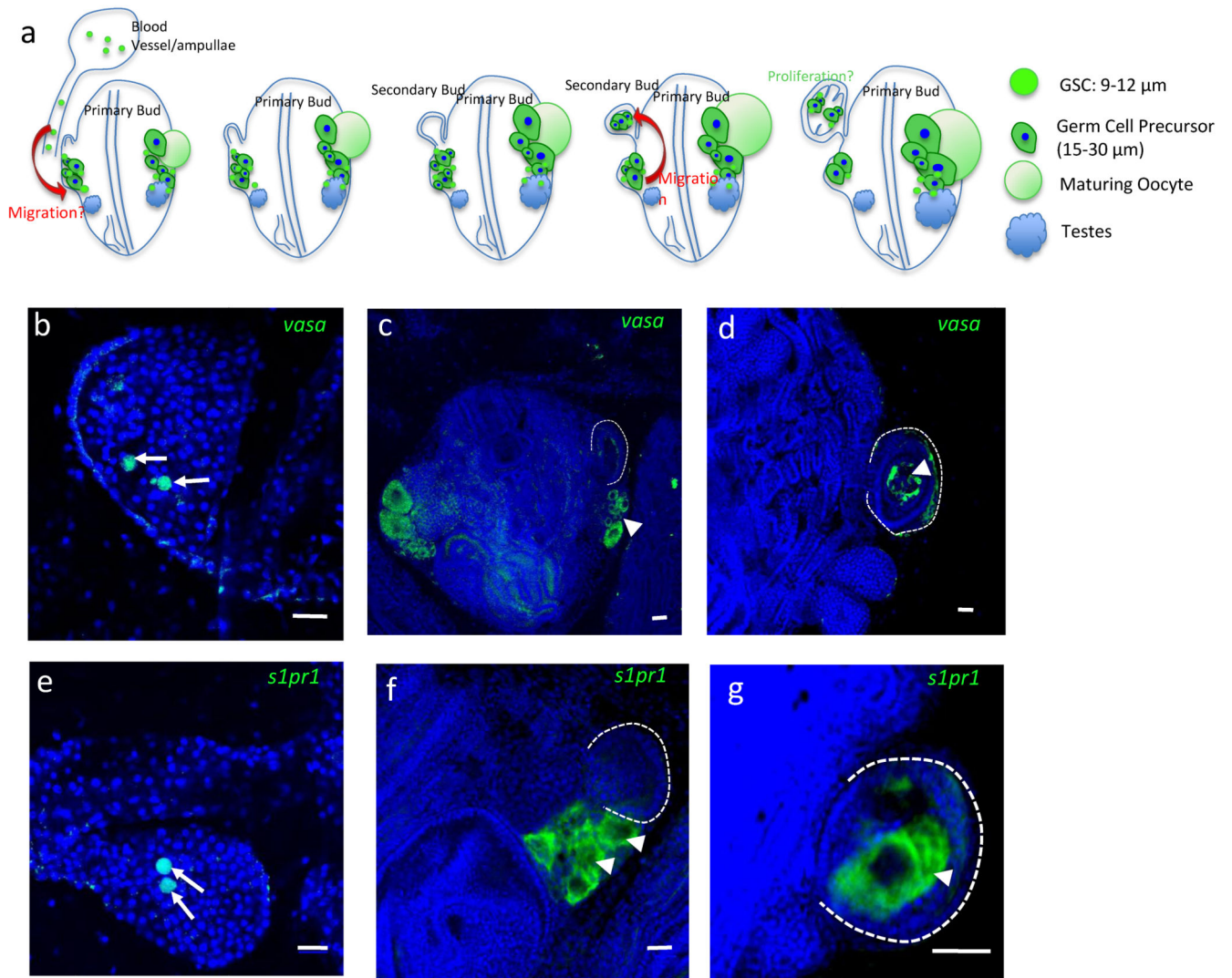


Figure 4. Mobile *vasa*- and *s1pr1*-positive germ cells migrate to secondary buds

a schematic representation of the in situ hybridization data presented in **b-g**. Small, round cells (7-10 μm diameter, green) expressing *vasa* and *s1pr1*, are present in the peripheral blood vessels, particularly in ampullae. At early stages of secondary bud development, these small *vasa/s1pr1*-positive germline stem cells (GSC) are also present inside the primary buds, in the vicinity of the developing gonads. We hypothesize that these small GSC that are present in the peripheral blood vessels enter into the primary bud by migration (red arrow), but the exact site and time point of entry is unknown. ... Larger germ cell precursors (15-30 μm , green), which also express *vasa*, *s1pr1*, likewise cluster around the gonads. When a secondary bud develops and closes to form a double vesicle, germ cell precursors (green) migrate into the secondary bud. As secondary bud development proceeds, more and larger germ cells are visible inside, indicating proliferation and differentiation. **b-g**) Representative images showing expression patterns of *vasa* and *s1pr1* by whole mount fluorescent in situ hybridization (green signal) merged with nuclear counterstaining (blue) (n=10). **b**) Round, small *vasa* (green) positive GSC inside an ampullae. **c**) *Vasa*-positive germ cells

(arrowhead) next to the developing secondary bud (broken white line). d) *Vasa*-positive germ cells (arrowhead) inside closed double vesicle secondary bud. e) Round, small *s1pr* (green) positive GSC inside an ampullae. f) *s1pr*-positive germ cells (arrowheads) next to the developing secondary bud (broken white line). g) *s1pr*-positive germ cells (arrowhead) inside closed double vesicle secondary bud. Nuclei were counterstained with Hoechst 33342 (blue). Note that small GSC in b and e have a high nuclear to cytoplasmic ratio. The blue signal from the nuclear counterstain overlying the green signal from the FISH appears turquoise. Scale bars = 20 μ m.

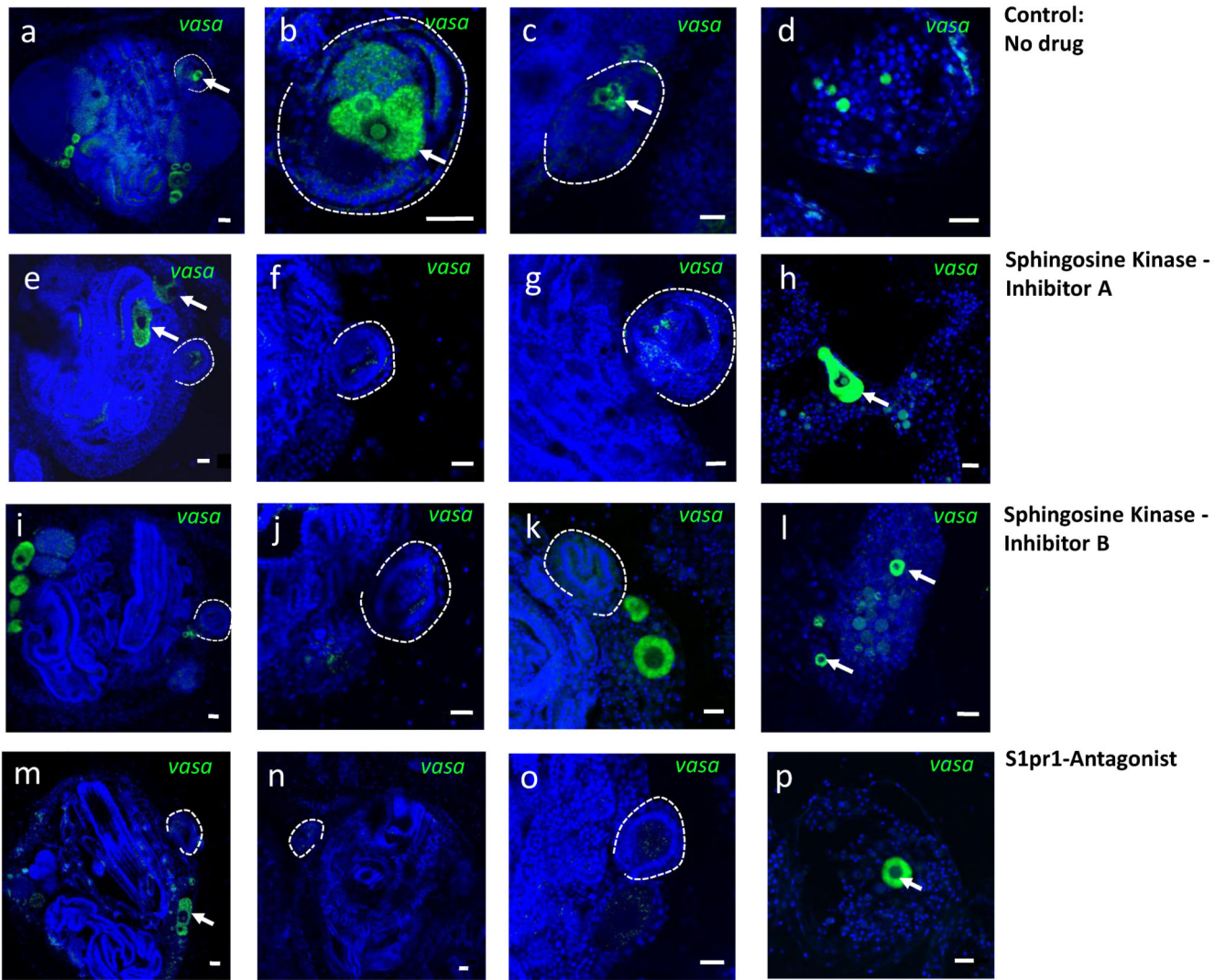


Figure 5. S1P signaling is essential for homing of germ cells into secondary buds

Animals were treated with Sphingosine Kinase inhibitors or S1PR1-antagonist for 3 days, starting at stage A1, and fixed at stage B2, when the secondary bud forms a closed double vesicle (n=4). Controls were left untreated. *Vasa*-FISH was performed on fixed animals, and localization of germ cells was analyzed by confocal microscopy. **a-c**) *vasa*-positive germ cells (green, arrows) homed into the double vesicle stage secondary bud (broken line) in a control animal. **d**) Ampulla of a control animal with *vasa*-positive GSC in the circulation. **e-h**) In animals treated with the sphingosine-kinase-inhibitor A (SK1-I), *vasa*-positive germ cells do not home to secondary buds (broken lines), but migrate randomly to other locations in the primary bud (**e**, arrow) and in the blood vessels (**h**, arrow). **i-l**) In animals treated with the sphingosine-kinase-inhibitor B (CAS 1177741-83-1), *vasa*-positive germ cells do not home to secondary buds (broken lines). Some larger *vasa*-positive germ cells remain outside of the closed double vesicle (**i** and **k**, arrows), while others are found in the blood vessels (**l**). **m-p**) In animals treated with S1PR1-antagonist, *vasa*-positive germ cells do not home to secondary buds (broken lines). Some larger *vasa*-positive germ cell precursors

randomly migrate in the vasculature. Nuclei were counterstained with Hoechst 33342 (blue).
Scale bars = 20 μ m.

Author Manuscript

Author Manuscript

Author Manuscript

Author Manuscript

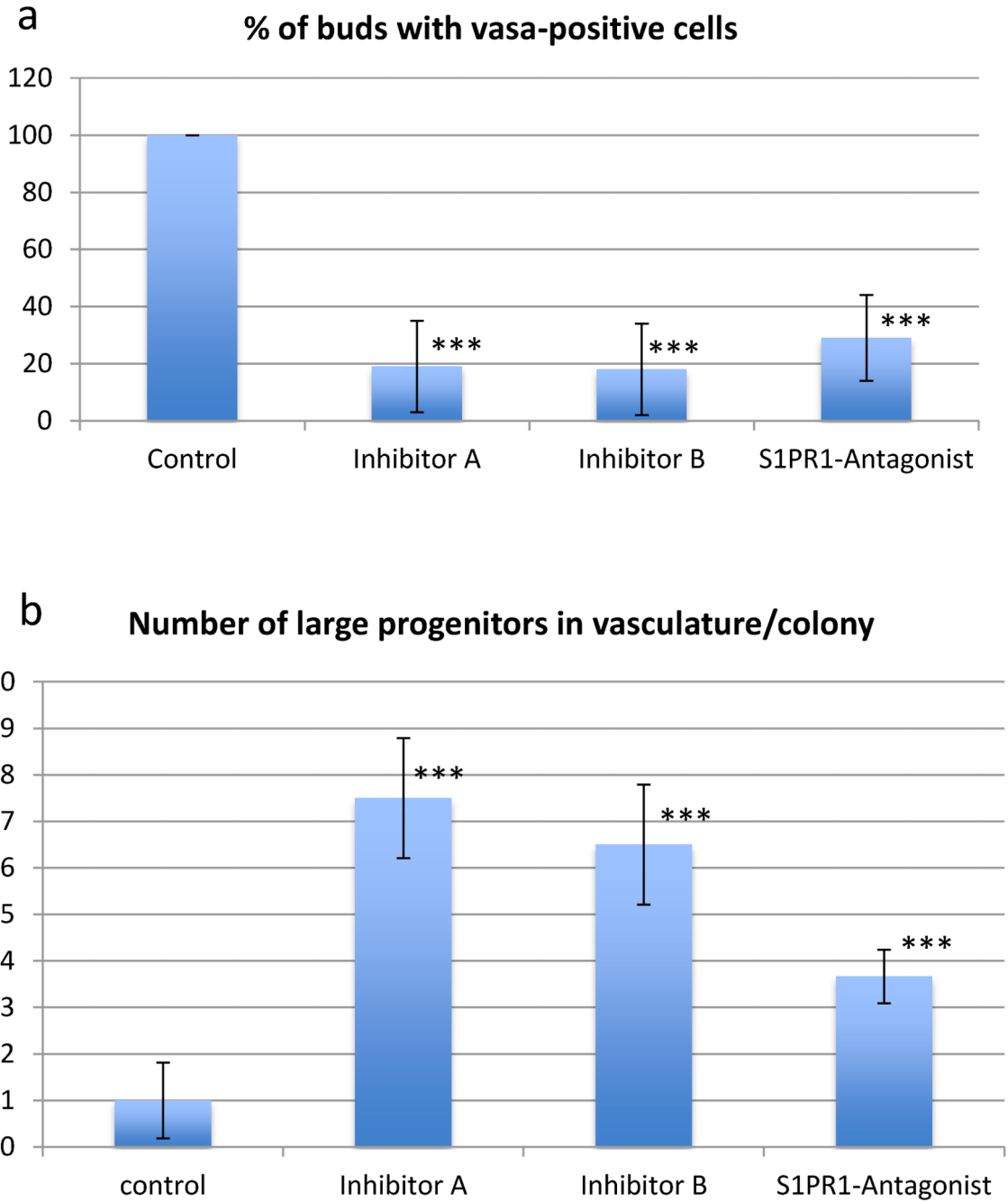


Figure 6. Quantification of migration defects in animals treated with inhibitors of S1P signaling
a) The number of double-vesicle-stage secondary buds containing *vasa*-positive were counted for each condition. Data are expressed as average percentages of buds containing *vasa*-positive cells, normalized to untreated controls. **b)** The number of large (>20 μ m) *vasa*-positive cells in the vasculature of the colony was counted for each condition. Data are expressed as average number of large *vasa*-positive cells per colony, normalized to untreated controls. Error bars represent the standard deviation for each average (n=4). Statistical

analysis was performed using Student's *t*-test. *** indicates $p < 0.01$ (high significance compared to control).

Author Manuscript

Author Manuscript

Author Manuscript

Author Manuscript

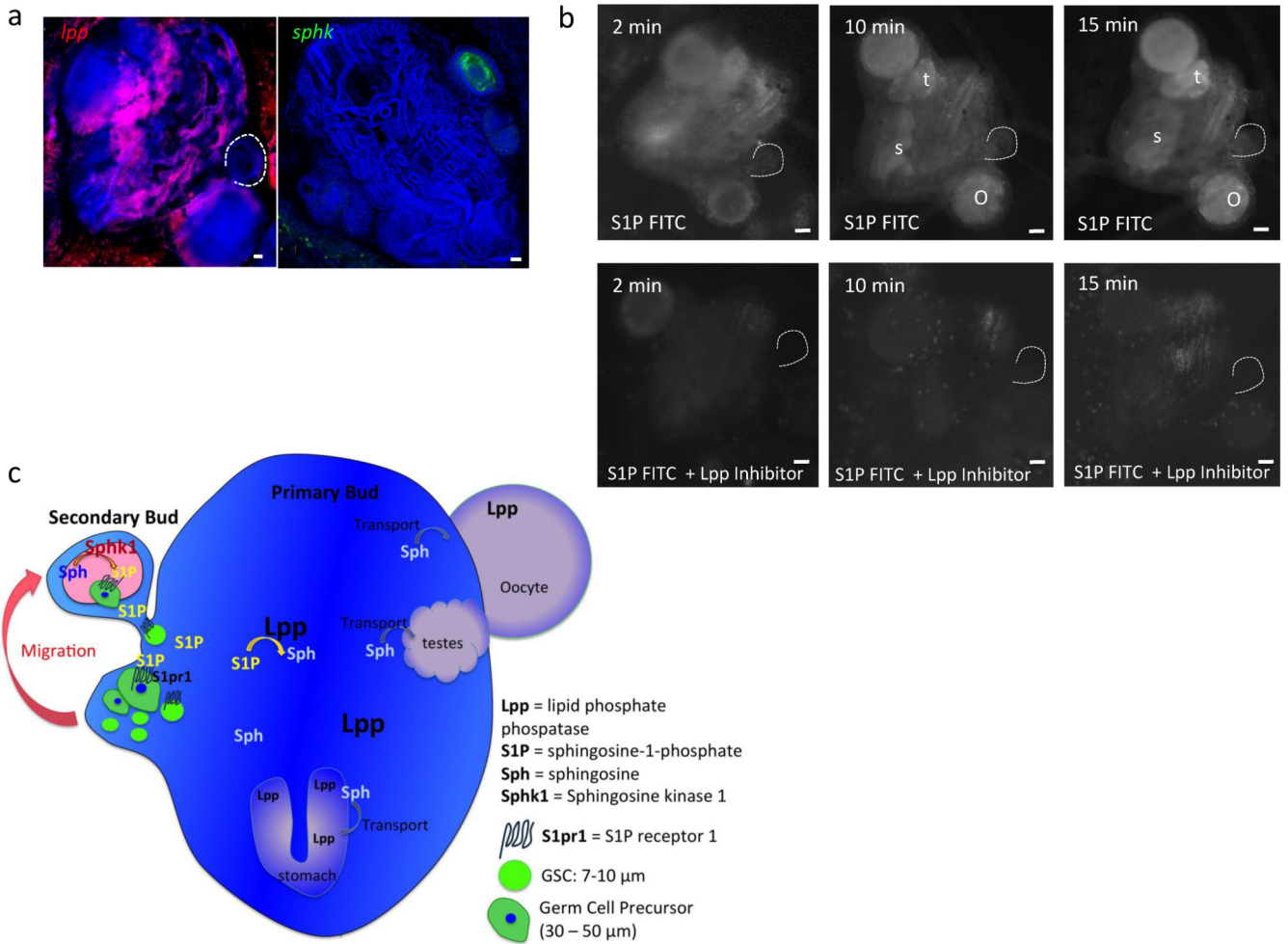


Figure 7. S1P is generated by sphingosine kinase in secondary buds and degraded by LPP in somatic tissues of the primary bud
a) FISH for *sphingosine kinase* (*sphk*, green) and *lipid phosphate phosphatase* (*lpp*, red). *Sphk* is expressed in double vesicle stage secondary buds, while *lpp* is expressed broadly in somatic tissues of the primary bud. Scale bars = 20µm. **b)** Live imaging of Fluorescence at different time points after injection of S1P-Fluorescein with or without the LPP inhibitor sodium-orthovanadate. After 10 minutes, S1P-Fluorescein accumulates in developing oocytes, testes and the stomach of the primary bud. This accumulation is inhibited by inhibition of LPP (n=3). Scale bars = 30µm **c)** Schematic summary of the in vivo data. Vasa-positive germ cells express S1PR1, and migrate towards a gradient of S1P into the germ cell niche in the secondary bud, where S1P is produced by Sphk. In somatic tissues of the primary bud, LPP dephosphorylates S1P to sphingosine, which then gets actively taken up by cells in the developing gonads and the stomach.